Electronic Supplementary Information(ESI)

for

Pyrene thiazole-conjugate as ratiometric chemosensor with high selectivity and sensitivity for tin (Sn^{4+}) and its application in imaging live cells

Ajit Kumar Mahapatra[*,a] Sanchita Mondal,[a] Kalipada Maiti,[a] Saikat Kumar Manna,[a] Rajkishor Maji,[a] Debasish Mandal,[b] Sukhendu Mandal,[c] Shyamaprosad Goswami,[a] Ching Kheng Quah[d] and Hoong-Kun Fun[d,e]

[a]Department of Chemistry, Indian Institute of Engineering Science and Technology, Shibpur, Howrah – 711103, India.

[b]Institute of Chemistry, The Hebrew University of Jerusalem, 91904 Jerusalem, Israel

[c] Department of Microbiology, Ballygunge Science College, Kolkata- 700019

[d] X-ray Crystallography Unit, School of Physics, Universiti Sains Malaysia, 11800 USM, Penang, Malaysia.

[e] Department of Pharmaceutical Chemistry College of Pharmacy, King Saud University, P.O. Box. 2457, Riyadh 11451 Kingdom of Saudi Arabia.

[*]Corresponding author: Tel.: +91 33 2668 4561; fax: +91 33 26684564;

E-mail: mahapatra574@gmail.com
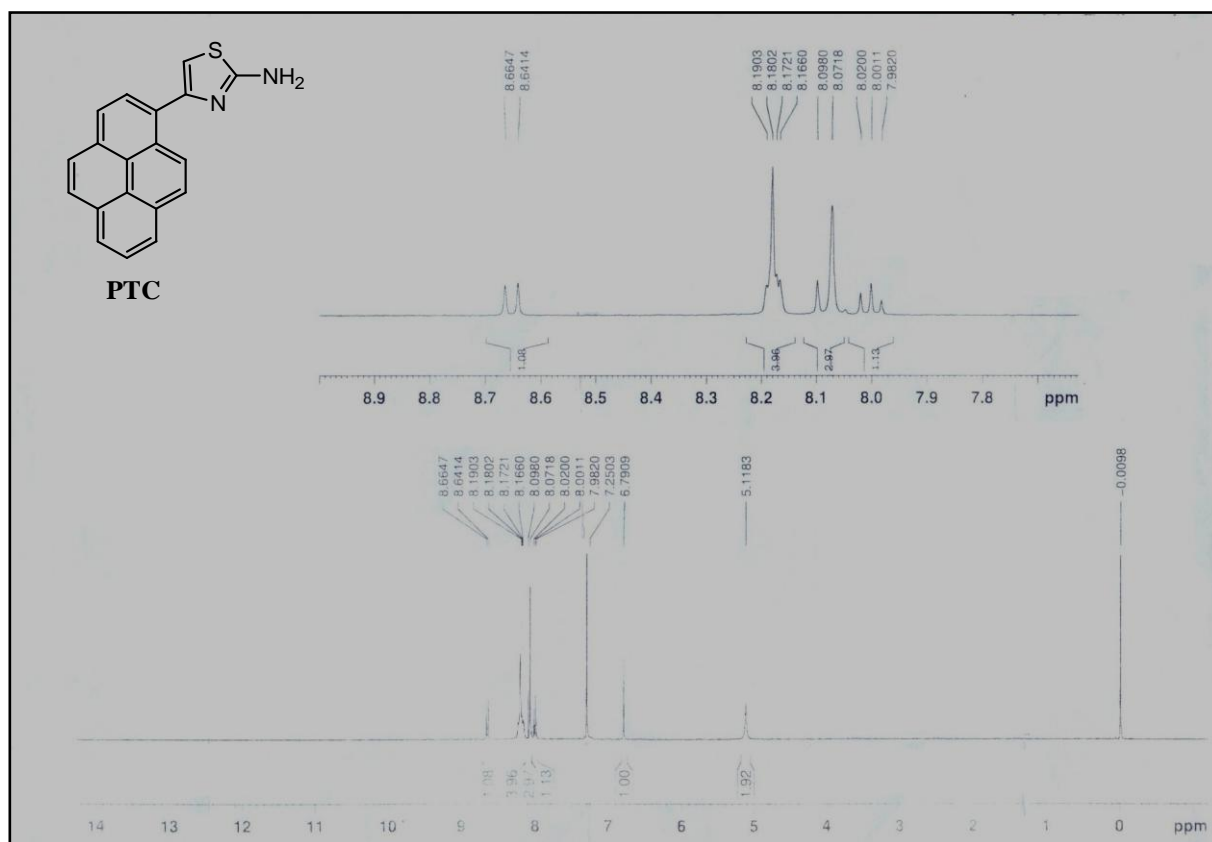
1. ^{1}H NMR spectrum of PTC (400 MHz, CDCl$_3$):

Figure S1: ^{1}H NMR spectrum of **PTC** in CDCl$_3$ solution.

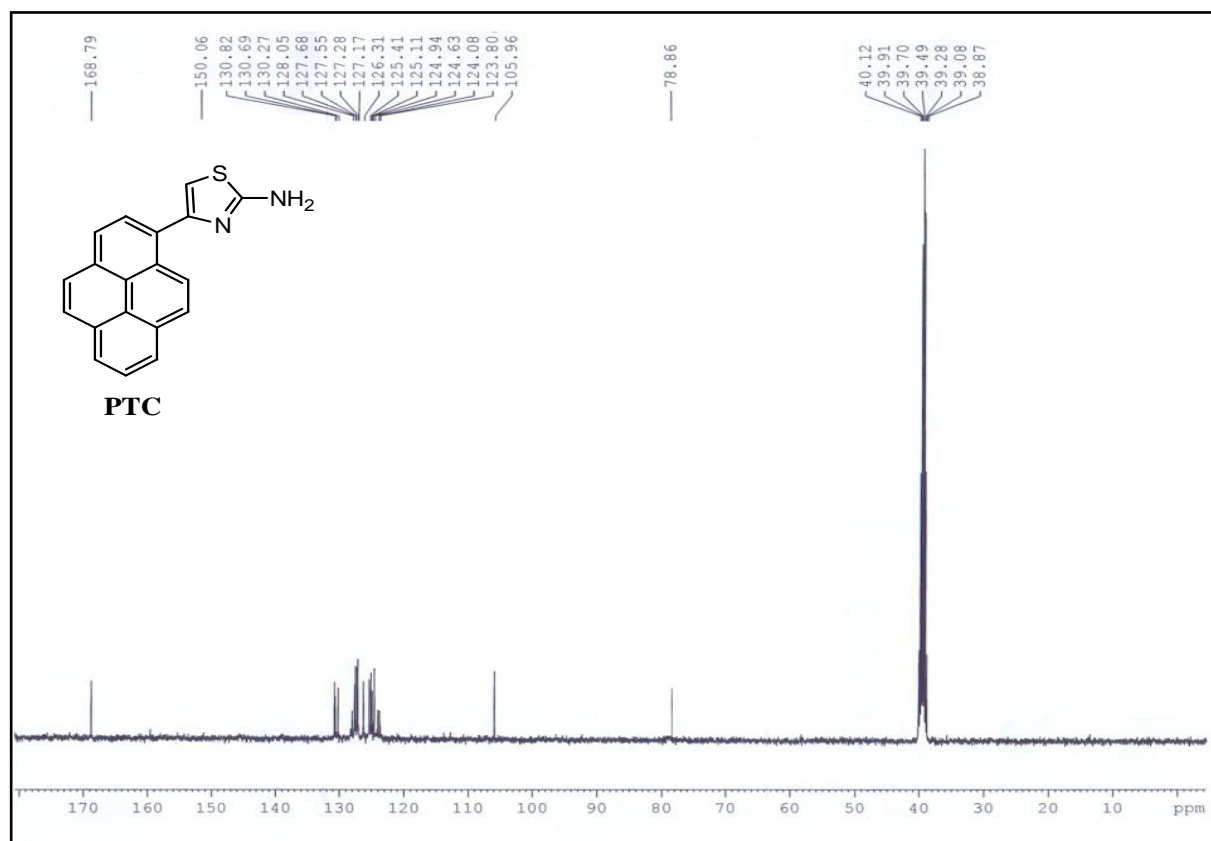## 2. ^{13}C NMR spectrum of PTC (400 MHz, d$_6$-DMSO):

Figure S2: ^{13}C NMR spectrum of **PTC** in d$_6$-DMSO solution.

3. TOF MS ES+ Mass Spectrum of PTC:
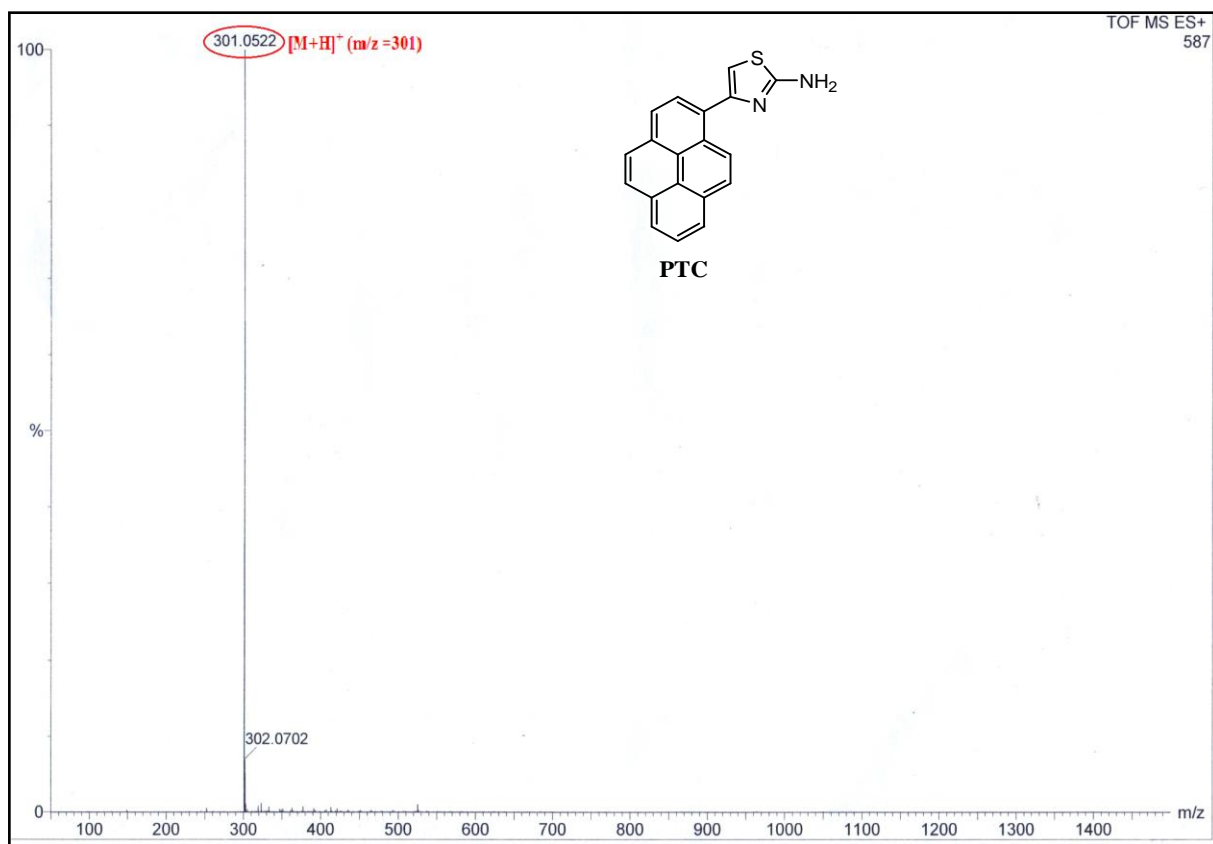
Figure S3: Mass spectrum of PTC.

4. ^{1}H NMR spectrum of PTC+SnCl$_4$.5H$_2$O (2-equivalent) +Na$_2$S (2-equivalent) in CDCl$_3$ solution:
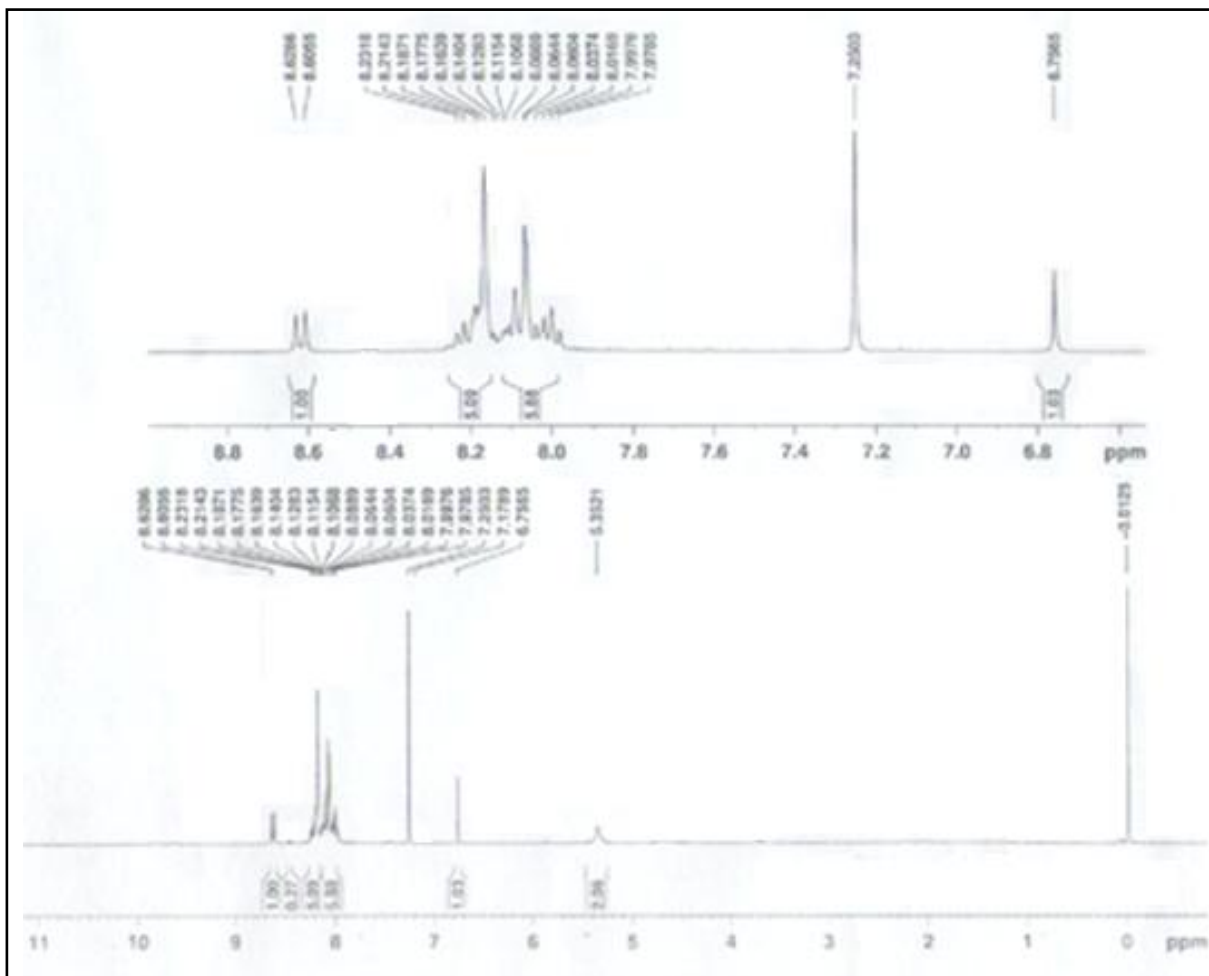
Figure S4: ^{1}H NMR spectrum of **PTC**+SnCl$_4$.5H$_2$O+Na$_2$S in CDCl$_3$ solution.

5. TOF MS ES+ Mass Spectrum of PTC in the presence SnCl₄.5H₂O:
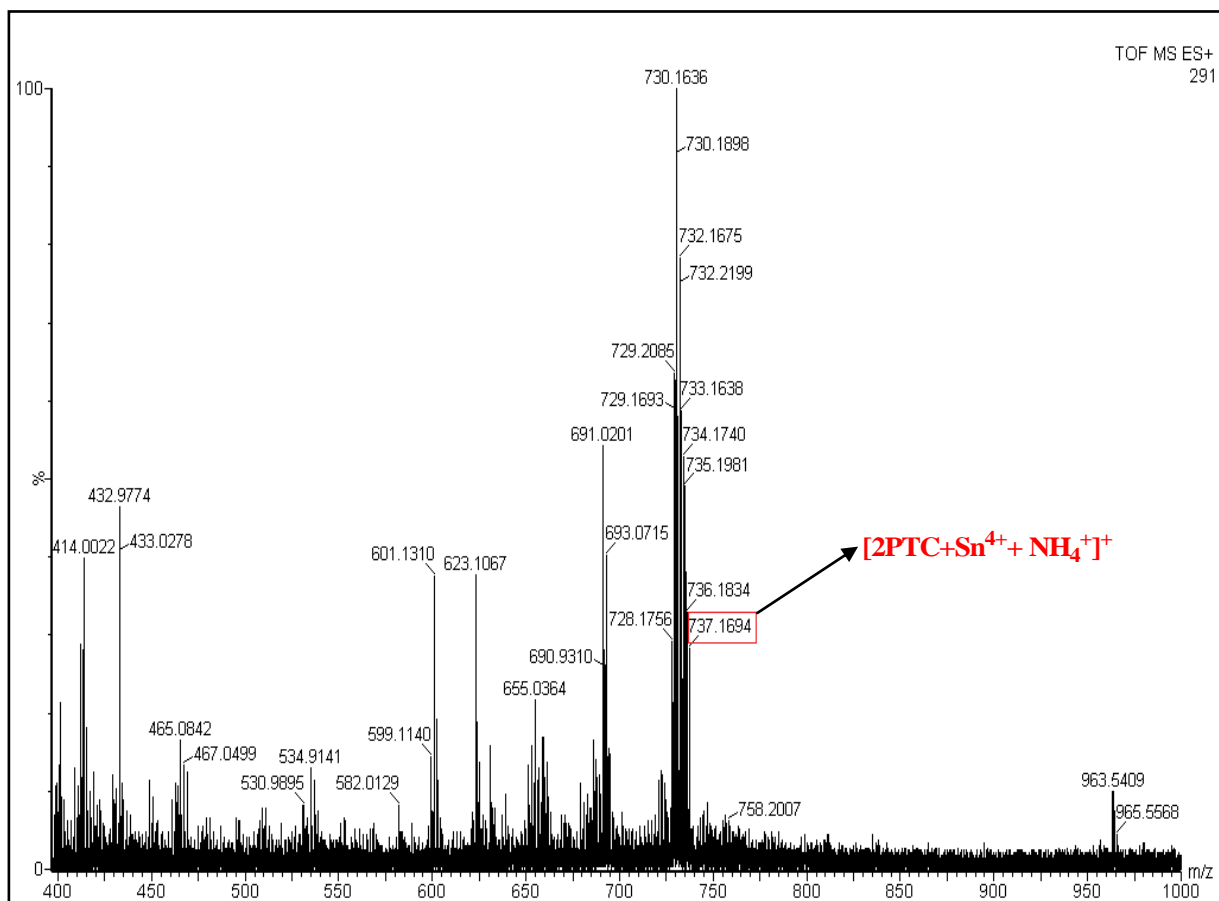
Figure S5: TOF MS ES+ Mass spectrum spectrum of **PTC**+Sn^{4+}.

6. TOF MS ES+ Mass spectrum of PTC+SnCl$_4$.5H$_2$O+Na$_2$S:
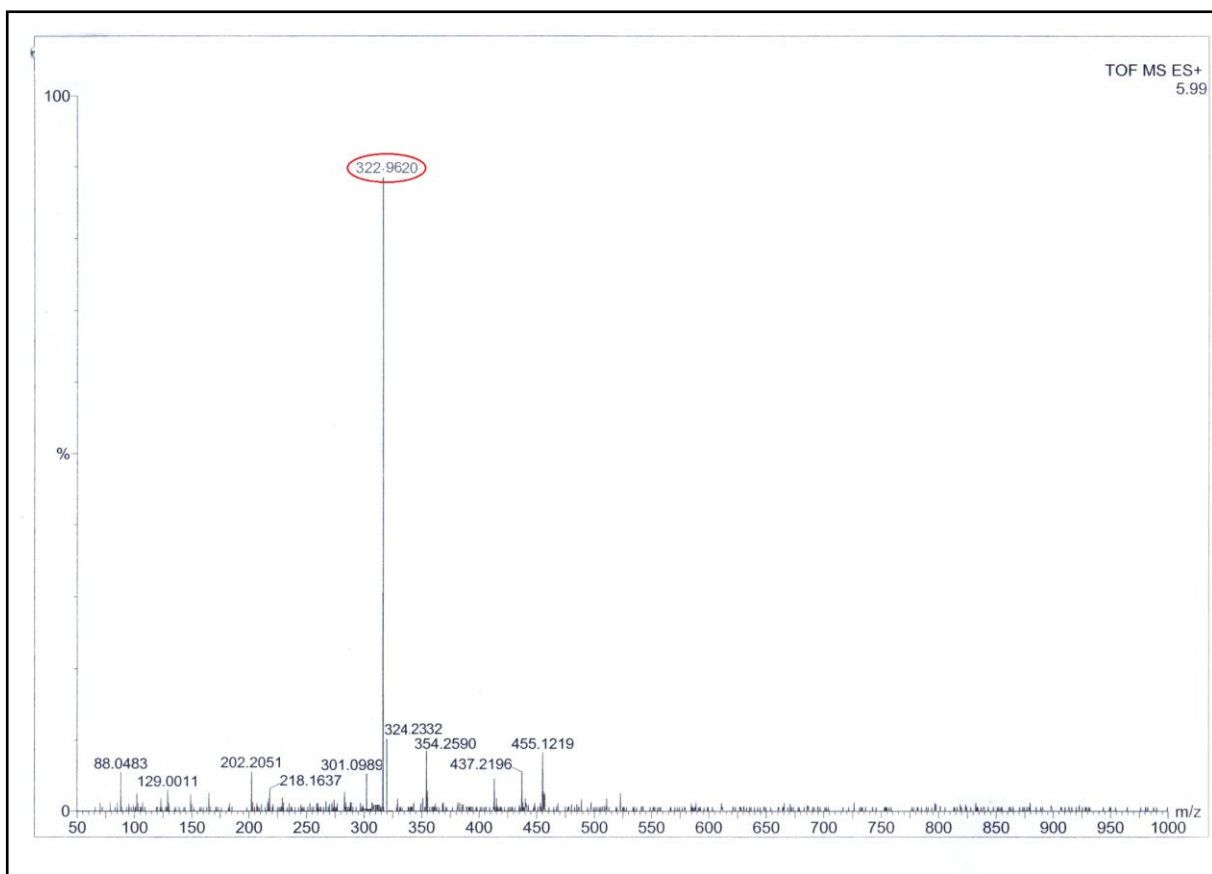
Figure S6: TOF MS ES+ Mass spectrum spectrum of **PTC**+Sn^{4+}+S^{2-}.

7. Job's plot for determining the stoichiometry of sensor PTC and Sn^{4+} ion by fluorescence method:

Figure S7: Job's plot of sensor **PTC** and Sn^{4+} ion by fluorescence method.

8. Visual and fluorescence photographic image of PTC in presence of different metal ions:

Figure S8: The Visible color (top) and fluorescence changes (buttom) of receptor **PTC** in EtOH–H$_2$O solution (EtOH : H$_2$O = 4 : 1, v/v, 10 mM HEPES buffer, pH = 7.4) upon addition of various metal ions.

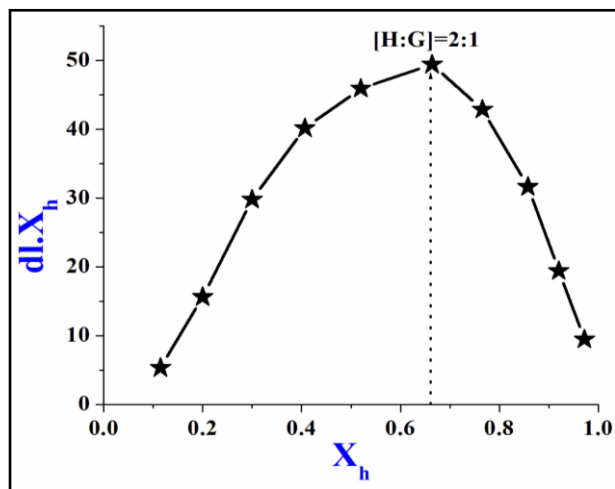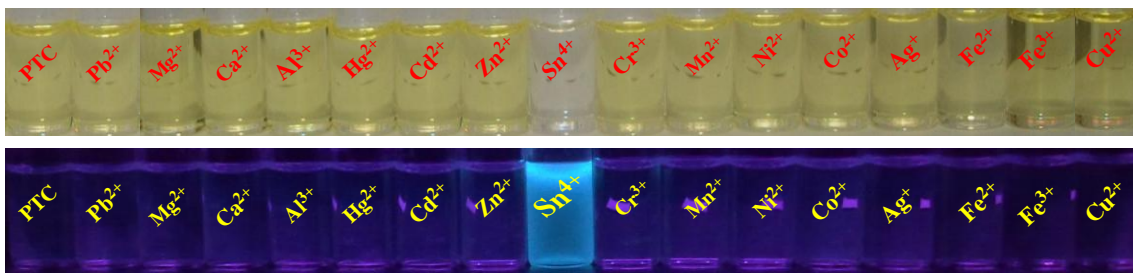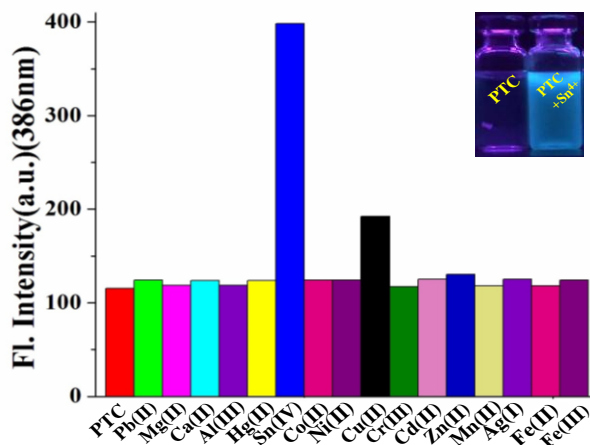## 9. Fluorescence Bar Diagram of PTC in presence of various metal ions:

Figure S9: Relative fluorescence changes (at 386 nm) of **PTC** (c = 4 × 10^{-5} M) , EtOH / H$_2$O = 4 : 1, v/v, 10 mM HEPES buffer, pH = 7.4) with respective metal cations (c = 2 × 10^{-4} M, left to right- PTC, Pb^{2+}, Mg^{2+}, Ca^{2+}, Al^{3+}, Hg^{2+}, Sn^{4+}, Co^{2+}, Ni^{2+}, Cu^{2+}, Cr^{3+}, Cd^{2+}, Zn^{2+}, Mn^{2+}, Ag^{+}, Fe^{2+}, Fe^{3+}. Fluorescence photograph of **PTC** and **PTC**+Sn^{4+}.

10. Evaluation of the Association Constant for the Formation of PTC·Sn^{4+}.

Receptor **PTC** with an effective concentration of 4×10^{-5} M in EtOH/H$_2$O solution (EtOH : H$_2$O = 4 :1, v/v, 10 mM HEPES buffer, pH = 7.4) was used for the emission titration studies with a Sn^{4+} solution. A stock solution of SnCl$_4$.5H$_2$O, having a concentration of 2×10^{-4} M in an aqueous HEPES buffer (4:1, v/v; pH 7.4) solution, was used.

Calculations for the Binding Constants Using Spectrophotometric Titration Data. The association constant and stoichiometry for the formation of the respective complexes were evaluated using the Benesi−Hildebrand (B−H) plot (eq 1).[1]

$$1/(I − I_0) = 1/K(I_{max} − I_0)[M^{n+}] + 1/(I_{max} − I_0) \qquad (1)$$

Here I_0, I_{max}, and I represent the emission intensity of free **PTC**, the maximum emission intensity observed in the presence of added metal ion at 386 nm, 402 nm, 485 nm for Sn^{4+} (λ_{ext} = 344 nm), and the emission intensity at a certain concentration of the metal ion added, respectively.

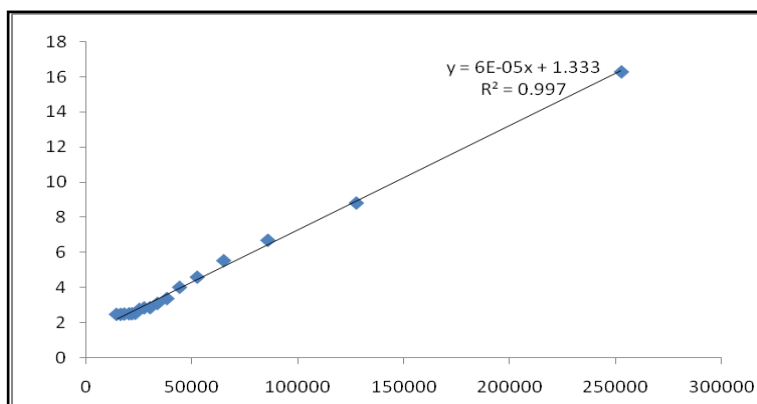## 10A. Association constant calculation graph (Absorption method):

Figure S10A: Bensei-Hildebrand plot obtained from absorption method (Excitation calculated from 344 nm) studies. Binding constant (K_a =2.22×10^4 M^{-1}) curve of sensor **PTC** with Sn^{4+} determined by UV-Absorbance method.

10B. Association constant calculation graph (Fluorescence method):
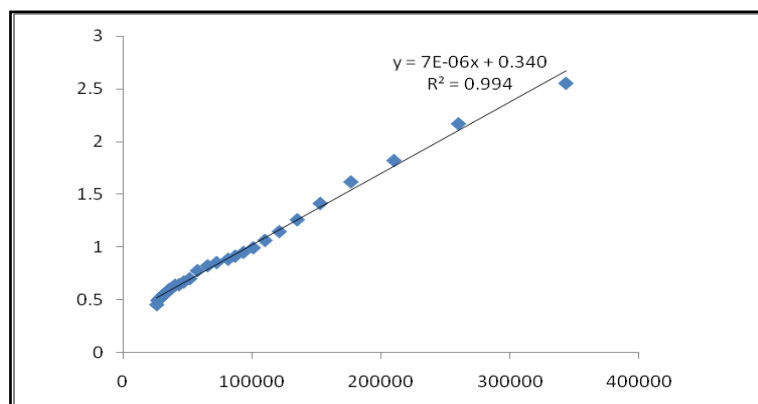
Figure S10B: Bensei-Hildebrand plot obtained from the Fluorescence (emmission calculated from 386 nm) studies. Binding constant (Ka = 4.86 × 10^4 M^{-1}) curve of sensor **PTC** with Sn^{4+} determined by fluorescence method.

11. Calculations for detection limit (Fluorescence method):

The detection limit (DL) of **PTC** for Sn^{4+} was determined from the following equation[2]:

DL = K* Sb1/S

Where K = 2 or 3 (we take 3 in this case); Sb1 is the standard deviation of the blank solution; S is the slope of the calibration curve.
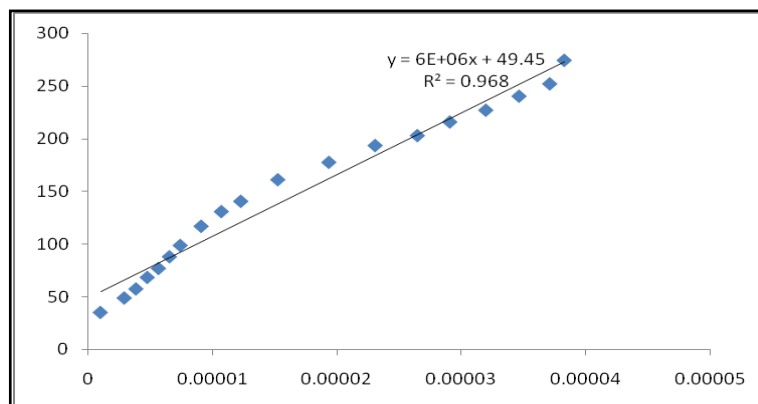
Figure S11. Calibration curve for fluorescence titration of **PTC** with Sn^{4+}.

From the graph we get slope (S) = 6×10^{6}. Standard deviation (Sb1=13.85817)

Thus using the formula we get the detection limit = 6.93 µM.

12. Reversibility Study:
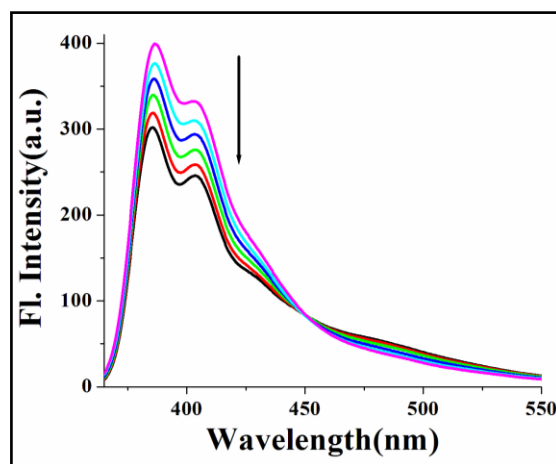
Figure S12: Change in fluorescence spectra of PTC-Sn^{4+} complex (c = 4×10^{-5} M) in EtOH–H_2O solution (EtOH : H_2O = 4 : 1, v/v, 10 mM HEPES buffer, pH = 7.4) upon addition of Na_2EDTA (c = 2×10^{-4} M).

13. Cytotoxicity Assay:

Figure S13: MTT assay to determine the cytotoxic effect of **PTC** and **PTC−Sn** complex on Vero 76 cells.

14. Computational Method:

Geometries have been optimized in B3LYP density functional method with 6-31G basis set for all atom excluding 6-31G* for sulphur and Lanl2dz for Sn. The geometries are verified as proper minima or not by frequency calculations. Time-dependent density functional theory calculation has also been performed at the same level of theory.
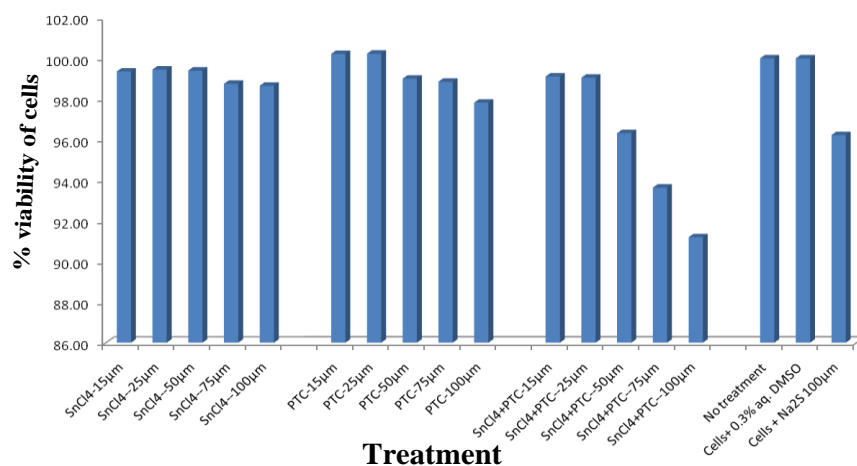
Selected electronic excitation energies (eV), oscillator strengths (f), main configurations, and CI Coefficients of the low-lying excited states of CS1 and all the complexes. The data were calculated by TDDFT//B3LYP/6-31+G(*d*) based on the optimized ground state geometries.

Molecules	Electronic Transition	Excitation Energy[a]	f^b	Composition[c]	(composition) %
PTC					
	$S_0 \rightarrow S_1$	3.3399 eV (371nm)	0.4119	$H \rightarrow L$ $H\text{-}1 \rightarrow L$	91.6
	$S_0 \rightarrow S_{15}$	5.3341 eV (232 nm)	0.3060	$H\text{-}2 \rightarrow L +3$ $H\text{-}3 \rightarrow L + 1$	40.5
	$S_0 \rightarrow S_{18}$	5.5644 eV (222 nm)	0.4839	$H\text{-}3 \rightarrow L + 1$ $H\text{-}3 \rightarrow L + 2$	65.3
		6.4775 eV (191 nm)	0.2809	$H\text{-}4 \rightarrow L + 3$	48.44
PTC-Sn^{4+}					
	$S_0 \rightarrow S_{18}$	3.0913 eV (401 nm)	0.4934	$H \rightarrow L +7$ $H \rightarrow L +4$	68.5

12

[a] Only selected excited states were considered. The numbers in parentheses are the excitation energy in wavelength. [b] Oscillator strength (only the f > 0.25 was considered). [c] H stands for HOMO and L stands for LUMO.

Species	E(HOMO)	E(LUMO)	ΔE	ΔE
PTC	-0.18581	-0.05670	3.513173477	81.01775155
Sn-PTC	-0.52398	-0.51621	0.211427139	4.875748815

15. X-ray crystallography study:

X-ray diffraction data of single crystals of **PTC** (with dimensions of 0.315×0.380×0.603 mm) was collected using Bruker APEX II Duo CCD area-detector diffractometer operating at 50kV and 30mA using Mo Kα radiation (λ = 0.71073 Å). Data collection and reduction were performed using the APEX2 and SAINT software.[3] The SADABS software was used for absorption correction. **PTC** was solved by direct method and refinement was carried out by the full-matrix least-squares technique on F^2 using SHELXTL package.[4] All non-hydrogen atoms were refined anisotropically whereas hydrogen atoms were refined isotropically. N-bound H atoms in **PTC** was located from the difference Fourier map and refined using a riding model with $U_{iso}(H)$ = 1.2 U_{eq} (N) [N—H = 0.8528 and 0.9053 Å]. The remaining H atoms were placed in calculated positions with C—H = 0.93 Å after checking their positions in the Fourier difference map. The U_{iso} values were constrained to be 1.2 U_{eq} of the carrier atom. The crystallographic data and hydrogen bonds geometry for **PTC** is presented in Table 1. Crystallographic data for **PTC** have been deposited with the Cambridge Crystallographic Data Center CCDC **1011198.**

Table S1: Experimental datails:

Crystal data	
CCDC number	**1011198**
Emperical formula	$C_{19}H_{12}N_2S$
M_r	300.37
Crystal system, space group	Monoclinic, $P2_1/c$
Temperature (K)	294
a, b, c **(Å)**	10.2235 (9), 12.4997 (11), 11.191 (1)
$\beta(°)$	100.6620(15)
V **(Å³)**	1405.4 (2)
Z	4
Radiation type	Mo $K\alpha$
μ **(mm^{-1})**	0.23
Crystal size (mm)	0.315×0.380×0.603
Data collection	
Diffractometer	Bruker *APEX* II DUO CCD area-detector diffractometer
Absorption correction	Multi-scan (*SADABS*; Bruker, 2009)
T_{min}, T_{max}	0.875, 0.932
Independent and observed [$I > 2\sigma(I)$] reflections	2346, 2346
θ **range (deg)**	2.5–26.0
hkl **range**	$h = -12 \rightarrow 12, k = -15 \rightarrow 15, l = -13 \rightarrow 13$
Refinement	
R_1, wR_2 **(%)**	0.040, 0.124
Completeness (%)	99.7
GOF (F^2)	1.04
H-atom treatment	isotropically

Table S2: Hydrogen-bond geometry (Å, °)

D—H$\cdots A$	D—H	H$\cdots A$	$D\cdots A$	D—H$\cdots A$
N2—H2*N2*$\cdots$**N1**[i]	0.91	2.10	3.002 (2)	174
C6—H6*A*$\cdots$**N1**	0.93	2.49	3.068 (2)	121

Symmetry code: (i) −*x*, −*y*, −*z*.

16. Calculation of quantum yield:

Here, the quantum yield ϕ was measured by using the following equation[5]:

$$\phi_x = \phi_s (F_x / F_s)(A_s / A_x)(n_x^2/ n_s^2)$$

Where,

X & S indicate the unknown and standard solution respectively, ϕ = quantum yield,

F = area under the emission curve, A = absorbance at the excitation wave length,

n = index of refraction of the solvent. Here ϕ measurements were performed using anthracene in ethanol as standard [ϕ = 0.28]

For standard (s) anthracene in ethanol the following values were determined:

n_s = 1.36 (for ethanol); F_s = 54369.64173; A_s = 0.315; ϕ_s = 0.28.

Here for **PTC**:

n_x = 1.36 (for ethanol); F_x = (area under the curve considering the region 360 nm-600 nm)12934.16422, A_x = 1.06.

ϕ_x(PTC)=0.0197.

For, **PTC**-Sn^{4+}:

n_x = 1.3617(for ethanol); F_x = (area under the curve considering the region 360 nm-600 nm) 22752.72347, A_x = 0.64;

ϕ_x(PTC-Sn^{4+})=0.0577.

Increase: 0.0577/0.0197= 2.93 fold of fluorescence quantum yield.

References:

1. (a) H. A. Benesi and J. H. Hildebrand, *J. Am. Chem. Soc.*, 1949, **71**, 2703−2707; (b) C. Yang, L. Liu, T. -W. Mu and Q. -X. Guo, *Anal. Sci.*, 2000, **16**, 537−539; (c) Y. Shiraishi, S. Sumiya, Y. Kohno and T. Hirai, *J. Org. Chem.,* 2008, **73**, 8571−8574.

2. (a) L. Long, D. Zhang, X. Li, J. Zhang, C. Zhang and L. Zhou, *Anal. Chim. Acta,* 2013, **775***,* 100–105; (b) M. Zhu, M. Yuan, X. Liu, J. Xu, J. Lv, C. Huang, H. Liu, Y. Li, S. Wang and D. Zhu, *Org. Lett.*, 2008, **10**, 1481-1484. (c) C. Kar, M. D. Adhikari, A. Ramesh and G. Das, *Inorg. Chem.,* 2013, **52**, 743−752.

3. Bruker. APEX2, SAINT and SADABS. Bruker AXS Inc.: Madison, WI, USA, 2009.

4. Y. Sheldrick, G.M. A short history of SHELX. *Acta Cryst.*, 2008, **A64,** 112-122.

5. K. Suzuki, A. Kobayashi, S. Kaneko, K. Takehira, T. Yoshihara, H. Ishida, Y. Shiina, S. Oishic, and S. Tobita. *Phys. Chem. Chem. Phys.*, 2009, **11**, 9850.